Interspeech 2025
17-21 August 2025, Rotterdam, The Netherlands

Functional Connectivity and Hilbert-Based Features for Covert Speech EEG Variability Analysis and Classification

Saravanakumar Duraisamy[1], *Maurice Rekrut*[2], *Luis A. Leiva*[1]

[1]University of Luxembourg, Luxembourg
[2]German Research Center for Artificial Intelligence (DFKI), Germany
saravanakumar.duraisamy@uni.lu, maurice.rekrut@dfki.de, luis.leiva@uni.lu

Abstract

We explore inter-trial, inter-class, and inter-subject variability in covert speech imagination using Electroencephalogram (EEG) signals. Two key functional connectivity metrics (Phase Locking Value and Coherence) revealed unique and shared activation patterns across speech commands, influenced by individual word perception and affective states. We also propose a subject-independent classification model using Hilbert envelope and instantaneous phase features across EEG frequency bands with a Bidirectional Long Short-Term Memory (BiLSTM) architecture, achieving 59.14% classification accuracy across five speech categories. Our state-of-the-art results in EEG-based speech decoding contribute a new understanding of the neural dynamics underlying imagined speech and affective processing.
Index Terms: speech decoding, electroencephalography, brain computer interfaces, deep learning

1. Introduction

Brain-Computer Interfaces (BCIs) enable direct communication between the brain and external devices by interpreting neural signals [1]. Among the various applications of BCIs, *covert speech* recognition, which involves decoding imagined speech from brain activity, has gained attention due to its potential to assist individuals with serious speech impairments such as locked-in syndrome [2, 3, 4]. Unlike overt speech, covert speech does not produce audible output, making its detection a really complex challenge.

While invasive techniques such as electrocorticography (ECoG), intracranial electroencephalography (iEEG), and neuroimaging modalities like magnetoencephalography (MEG) have shown remarkable performance in decoding imagined speech [5], they come with limitations in terms of cost, portability, and comfort [6]. In contrast, electroencephalography (EEG) offers a non-invasive, wearable, and user-friendly approach, making it well-suited for real-world BCI applications, despite its low spatial resolution and susceptibility to noise.

Recent advancements in EEG technology have demonstrated the feasibility of BCIs for recognizing imagined speech, yet classification accuracy remains a major obstacle, limiting their real-world implementation [7, 8]. One of the primary challenges in covert speech EEG analysis is the high variability across trials and subjects. Neural responses to imagined speech are influenced by cognitive differences, mental rehearsal strategies, and background neural noise, leading to high inter-subject variability in recorded EEG patterns. Addressing this variability is crucial for improving the reliability of BCIs.

Previous work [9, 10, 11, 12] explored various feature extraction and classification techniques to enhance EEG signal decoding, yet most approaches struggle to generalize across different users and recording sessions. To address these limitations, recent research has investigated functional connectivity (FC) measures as a means of identifying stable neural interactions during covert speech [13]. FC-based metrics, such as phase synchronization and coherence, offer insights into the underlying neural mechanisms by analyzing how different brain regions communicate during imagined speech processes [14, 15]. Additionally, time-frequency analysis techniques have been explored to extract meaningful features from EEG signals, capturing both spectral and temporal characteristics of brain activity [16, 17, 18].

Despite these advancements, the challenge of improving classification performance while mitigating inter-trial, inter-class and inter-subject variability remains largely unresolved. Further investigation is needed to refine feature extraction methods, optimize classification models, and establish robust strategies for enhancing EEG-based covert speech decoding. To address these challenges, this study explores inter-trial, inter-class, and inter-subject variability in covert speech EEG using FC metrics. We develop a subject-independent classification model using Hilbert-based features and a BiLSTM network to enhance EEG-based speech decoding.

2. Methodology

2.1. Datasets

Two datasets were utilized for this study. The **BCI Competition 2020** dataset [19] comprises 15 subjects EEG recordings of imagined speech for five different words: 'hello', 'help me', 'stop', 'thank you', and 'yes'. The dataset consists of 80 trials per class ($80 \times 5 = 400$ trials), with 60 trials per class used for training, and 20 trials per class designated for validation and testing. The EEG signals were recorded using a 64-channel (Figure 1) EEG system[1] (BrainAmp, Brain Products GmbH, Germany) at a sampling frequency of 500 Hz, following the 10-10 international EEG system. The recordings were captured during imagined speech tasks, where participants were instructed to imagine speaking without producing any overt vocalization. The imagined speech phase in the experiment was set to 2 seconds per trial, and the dataset was divided into epochs based on cue information for analysis.

The **Overt/Covert** dataset [20] comprises EEG recordings from 15 healthy, right-handed subjects (11 male, 4 female, average age 26.8 years) who performed both covert (imagined) and overt (spoken) speech tasks. The data were collected in a controlled environment while participants interacted with a robot. The experiment involved five command words: LEFT, RIGHT,

[1]https://brainvision.com/products/brainamp-standard/

10.21437/Interspeech.2025-1986

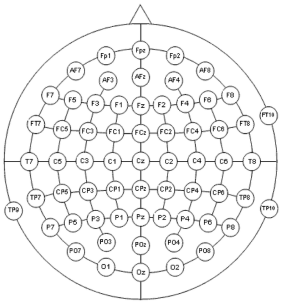

Figure 1: *64-channel EEG topographical locations.*

UP, PICK, and PUSH. Each session consisted of eight levels, with each level containing five repetitions of each word. The data were recorded with a 64-channel wireless EEG system[2] (Brain Products LiveAmp 64) at a sampling rate of 500 Hz, following the 10-10 international EEG system. Similar to the BCI Competition 2020 Dataset, the imagined speech phase for each trial was also set to 2 seconds.

2.2. EEG preprocessing

For both datasets, a consistent pre-processing pipeline was applied to prepare the data for analysis and feature extraction. First, a 50 Hz notch filter was applied to eliminate powerline interference. Subsequently, a 5th-order Butterworth Finite Impulse Response (FIR) filter with a passband of 0.5–80 Hz was used to filter the EEG signal, retaining relevant frequency components while removing unwanted noise. To address artifacts associated with eye blinks, muscle movements, and other non-neural activities, independent component analysis (ICA) was employed on the filtered EEG data [21].

The EEG signals were divided into two-second epochs, aligning with the speech production phase in both datasets. A 100 ms pre-stimulus window was applied for baseline correction, where the mean signal from this window was subtracted from each epoch. This process helped eliminate baseline drift and enhance signal consistency across trials. After preprocessing, each trial was labeled according to the covert speech task, and the data from each dataset were processed separately.

2.3. EEG signal analysis

To explore brain activity variability during speech imagination, we analyzed **inter-trial**, **inter-class**, and **inter-subject** differences using two key FC metrics [22, 23]: Coherence and Phase Locking Value (PLV).

On the one hand, **Coherence** quantifies the linear correlation between two signals across different frequency bands, indicating neural synchrony. On the pother hand, **PLV** measures phase synchronization between signals, reflecting the consistency of phase relationships across trials.

For **inter-trial variability**, we first calculated the ensemble average EEG for each speech class (e.g., 'hello', 'thank you') within a subject. This average served as a reference for that class. We then computed the two metrics (Coherence and PLV) between individual trials and their corresponding reference to assess the variability in neural responses for the same word across different trials.

[2] https://brainvision.com/products/liveamp-64/

To analyze **inter-class variability**, we computed a graded average EEG across all speech trials within a subject, irrespective of class. The class-specific averages were then compared to this graded average EEG using the two metrics. This analysis quantifies how each imagined word differs from the subject's overall neural activity pattern.

For **inter-subject variability**, we first computed the class-specific average EEG for each participant, resulting in five matrices per subject (one for each word). We then calculated the graded average EEG for each class across all participants, yielding five global matrices. The two metrics were then computed between each participant's class-specific EEG and the corresponding global class average. This analysis quantified how the neural representation of the same word varied across individuals compared to the collective pattern observed in all participants.

2.4. Feature extraction and classification model

We use Hilbert Envelope (ENV) and Temporal Fine Structure (TFS) from EEG signals as relevant features for imagined speech decoding, following previous work [24]. ENV captures amplitude fluctuations linked to speech activity, while TFS encodes phase information crucial for modeling neural dynamics. For each trial, ENV and TFS features are derived from EEG segments of size 1000×C, where C is the number of channels. Both representations retain the original dimensions and are concatenated along the feature axis, yielding a final input of size $1000\times 2C$.

We adopt a subject-independent classification strategy using a bidirectional long short-term memory (BiLSTM) network. Each participant provides 80 EEG trials per covert speech class. The model input is a 3D tensor of shape $(B, 1000, F)$, where $B = 32$ is the batch size, 1000 denotes the number of time steps, and F is the feature dimension (twice the number of EEG channels due to ENV-TFS concatenation). The network is trained using the Adam optimizer with a learning rate $\eta = 0.0001$ and decay parameters $\beta_1 = 0.9$, $\beta_2 = 0.999$. Categorical cross-entropy is used as the loss function for multi-class classification. The full BiLSTM architecture is detailed in Table 1.

Table 1: *BiLSTM model configuration.*

Layer	Params	Details
Input	None	Shape: (B, 1000, F)
BiLSTM 1	Input: 4×F×512 Recur.: 4×512×512 Bias: 4×512	512 units, tanh activation Dropout: 0.3
BiLSTM 2	Input: 4×1024×256 Recur.: 4×256×256 Bias: 4×256	256 units, tanh activation Dropout: 0.2
FC	Weights: 256×5 Bias: 5×1	Output: 5 classes
Output	None	Softmax activation

3. Results and Discussion

3.1. EEG variability analysis

Inter-trial analysis during speech imagination serves to assess the consistency of speech-related EEG channel activation across multiple trials. This analysis is crucial for identifying the

most relevant EEG channels for constructing an optimal classifier. Unlike steady-state visually evoked potentials (SSVEP) or P300-based BCIs [25], where well-defined channel locations are established, imaginary speech-based BCIs lack standardized optimal electrode positions. Thus, understanding FC patterns can guide channel selection efficiently.

Figure 2 illustrates the PLV and coherence-based inter-trial variability analysis of the first two trials of same word imagined by a single subject in the Overt/Covert dataset. Similar patterns were observed in the BCI Competition 2020 dataset. Each heatmap represents FC between an individual trial and the ensemble average of a given class. The diagonal elements in the heatmaps denote connectivity measures between the same channel in the reference and trial EEG data. The off-diagonal indicates the connectivity measures across channels. A PLV or Coherence value close to 1 suggests a high degree of correlation, indicating nearly identical signals.

Channels located in the inferior frontal gyrus (F7, F8, F5, F6), superior temporal gyrus (T7, T8, TP7, TP8), and premotor cortex areas (FC5, FC1, FC2, FC6, FC3, FC4) are involved in speech production and perception, exhibiting consistent FC across trials. Beyond these primary regions, enhanced connectivity was also observed in fronto-central, central, temporal, parietal, and occipito-parietal areas (F3, Fz, F4, FC1, FCz, FC2, C1, Cz, C2, CP1, CPz, CP2, CP3, CP4, CP5, CP6, P3, Pz, P4, P5, P6, P7, P8, PO3, POz, PO4, PO7, PO8), mostly attributed to cognitive processing and sensorimotor integration during speech imagination. These locations were selected using a PLV threshold of 0.604, determined via a Gaussian Mixture Model (GMM) clustering analysis [26]. This threshold reflects a statistically significant boundary between low and high connectivity groups ($t = 700.25$, $p < .0001$).

To examine variability across different imagined words, we conducted an inter-class analysis using the same FC metrics described in Section 2.3. Figure 3 presents topographical representations of the diagonal elements from the PLV matrix in the Overt/Covert dataset, which indicate channel-wise connectivity between the reference and class-specific EEG signals. Again, similar patterns were observed in the BCI Competition 2020 dataset.

Interestingly, we observed common activation patterns across different imagined words within speech perception and speech production areas. However, additional activation patterns emerged in central, frontocentral, parietal, and occipitoparietal regions, suggesting that imagined speech involves more than just motor execution—it engages multimodal processing and semantic networks. Previous studies [27, 28, 29] have linked these regions to affective processing, suggesting that different imagined words may evoke distinct affective and cognitive responses. We can conclude that speech imagination is not solely constrained to speech production mechanisms. Our results indicate a strong association with speech perception and affective states, aligning with neurocognitive models of language processing.

To further investigate inter-subject differences in speech imagination, we examined FC patterns across subjects imagining the same word. Figure 4 illustrates PLV of same word of three subjects, demonstrating that while core speech-related regions remain active, subject-specific differences emerge in above mentioned activation areas. This suggests that subjective interpretation, prior experience, and individual affective responses play a role in how speech imagination is represented in the brain [27, 29].

3.2. Classification experiments

Few studies have explored subject-independent and cross-subject models in covert speech BCIs [30, 31]. Most existing studies focus on subject-specific models without exploring speech variability across different words, trials, and subjects. Therefore, our study significantly progresses beyond the state of the art. Prior to classification, each subject's EEG data is normalized independently using Z-score based on their own data.

Our previous analysis in Section 2.3 has identified active EEG brain regions involved in speech imagination, suggesting that affective perception plays a significant role. Based on this analysis, we selected 42 active EEG channels as optimal channels and subject's perceptual features for classification. Then, we developed three different classifiers, all using Hilbert-based EEG features as input.

Model 1 utilized EEG signals from 64 channels. The ENV and TFS features were extracted for each trial. Each EEG segment originally had a dimension of 1000×64. After feature extraction (ENV and TFS) the segments were concatenated horizontally, resulting in a final dimension of 1000×128.

Model 2 used EEG signals from the 42 selected channels. Similar to the first model, ENV and TFS features were extracted, leading to an initial dimension of 1000×42, which was then transformed into 1000×84 after concatenation.

Model 3 was developed based on our previous analysis, considering that affective responses are EEG band-specific [32]. The selected 42-channel EEG data was bandpass filtered into three frequency bands by using filter bank decomposition: low-frequency (0.5 to 8 Hz), medium-frequency (8 to 30 Hz), and high-frequency (30 to 80 Hz). The filtered EEG data from all three bands were concatenated, resulting in a total trial dimension of 1000×126. After applying ENV and TFS, the final feature dimension of a single trial became 1000×252.

Since we used two different datasets, we implemented six subject-independent models using 10-fold cross validation, to ensure generalizability across individuals. The classification accuracy of subject-independent models is reported in Table 2, demonstrating the impact of feature selection and frequency decomposition.

Table 2: *Subject-independent classification accuracy.*

Dataset	Model 1	Model 2	Model 3
D1 [19]	33.48 ± 4.74	38.15 ± 5.32	56.22 ± 4.48
D2 [20]	30.63 ± 5.21	40.69 ± 3.89	59.14 ± 4.32

Model 1, which used EEG signals from all 64 channels, achieved the lowest accuracy. This suggests that including all channels without proper selection actually introduces noise. Model 2, utilizing the 42 most active EEG channels, improved accuracy to 38.15% for D1 and 40.69% for D2, indicating the effectiveness of channel selection in enhancing classification performance. Model 3, which incorporated EEG band-specific filtering before feature extraction, achieved the highest accuracy. This highlights the importance of frequency-specific information in imagined speech classification. Our results confirm that both channel selection and frequency-based decomposition significantly enhance classification accuracy, validating the role of affective perception and EEG spectral features in subject-independent imagined speech modeling.

We also implemented a cross-subject model with 15-fold validation, where in each fold the data from one subject is used

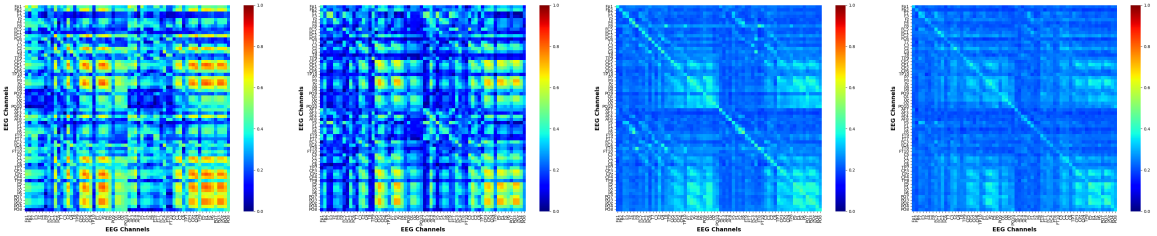

(a) *Trial 1: PLV* (b) *Trial 2: PLV* (c) *Trial 1: Coherence* (d) *Trial 2: Coherence*

Figure 2: *Heatmap of inter-trial analysis of FC measures in the Overt/Covert dataset.*

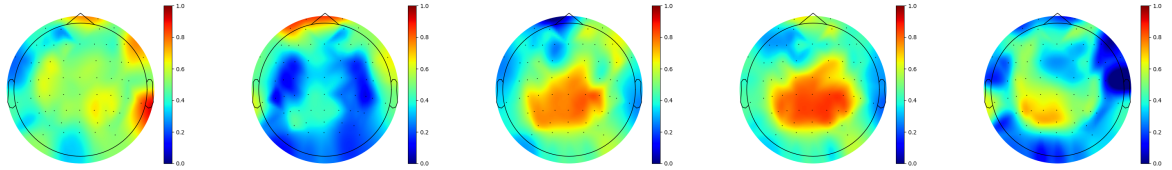

(a) *Class: UP* (b) *Class: PICK* (c) *Class: LEFT* (d) *Class: RIGHT* (e) *Class: PUSH*

Figure 3: *Topoplot of PLV representing inter-class variability across different imagined speech classes in the Overt/Covert dataset.*

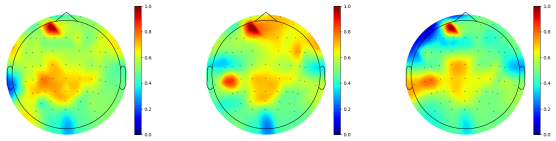

(a) *Subject 1* (b) *Subject 2* (c) *Subject 3*

Figure 4: *Topoplot of PLV representing inter-subject variability across the imagined speech word 'thank you' in the BCI Competition 2020 dataset.*

Table 3: *Cross-subject classification accuracy.*

Dataset	Model 1	Model 2	Model 3
D1 [19]	19.35 ± 3.42	21.78 ± 3.11	25.62 ± 4.85
D2 [20]	18.41 ± 3.78	22.63 ± 4.05	27.15 ± 3.92

for testing. The results are reported in Table 3. As observed, cross-subject models perform poorly, with Model 1 achieving near-random accuracy, and Model 2 and 3 performing slightly above random. These results suggest that cross-subject modeling is ineffective for imagined speech classification, likely due to the unique individual differences in speech perception and imagination [27]. Since each subject internally processes words differently, based on their cognitive and emotional states, a subject-independent model struggles to generalize across individuals. Furthermore, the proposed model is compared with an existing subject-independent model, as illustrated in Table 4. Compared to the state-of-the-art (SOTA) models, our proposed model[3] achieves higher performance.

[3] https://doi.org/10.5281/zenodo.15555946

Table 4: *Comparison against previous work, sorted by year.*

Ref.	No. commands	Accuracy (%) ± SD
[33]	6	19.68
[7]	6	31.40 ± 2.73
[34]	5	48.10 ± 3.68
[30]	4	49.93 ± 1.72
[31]	6	34
[35]	4	45
[15]	3	44.2
Ours	5	**59.14 ± 4.32**

Refs [33, 31, 35, 15] did not report SDs.

A major limitation of this study is the inability of cross-subject models to learn subject-specific information critical for accurate classification. Future work should focus on hybrid approaches, such as transfer learning or meta-learning, to adapt a generalized model to individual subjects with minimal fine-tuning. Additionally, incorporating advanced modeling techniques such as attention mechanisms or subject-specific embeddings, may help models better capture personalized patterns.

4. Conclusion

Our study reveals the complexities of inter-trial, inter-class, and inter-subject variability in EEG signals during covert speech imagination, highlighting the key role of affective states in speech perception and production. Our subject-independent BiLSTM model sets a new SOTA, further underscoring the value of FC metrics, channel selection, and frequency-specific features in improving EEG-based speech decoding. The findings also highlight limitations of cross-subject models, which struggle to capture individual neural differences.

5. Acknowledgements

Research supported by the European Innovation Council's Pathfinder program (SYMBIOTIK project, grant 101071147) and the German BMBF (grants 01IS12050 and 01IS23073).

6. References

[1] J. R. Wolpaw, N. Birbaumer, D. J. McFarland, G. Pfurtscheller, and T. M. Vaughan, "Brain–computer interfaces for communication and control," *Clinical neurophysiology*, vol. 113, no. 6, 2002.

[2] J. T. Panachakel and A. G. Ramakrishnan, "Decoding covert speech from eeg-a comprehensive review," *Frontiers in Neuroscience*, vol. 15, 2021.

[3] D. Lopez-Bernal, D. Balderas, P. Ponce, and A. Molina, "A state-of-the-art review of eeg-based imagined speech decoding," *Frontiers in human neuroscience*, vol. 16, 2022.

[4] N. Rahman, D. M. Khan, K. Masroor, M. Arshad, A. Rafiq, and S. M. Fahim, "Advances in brain-computer interface for decoding speech imagery from eeg signals: a systematic review," *Cognitive Neurodynamics*, 2024.

[5] F. R. Willett, E. M. Kunz, C. Fan, D. T. Avansino, G. H. Wilson, E. Y. Choi, F. Kamdar, M. F. Glasser, L. R. Hochberg, S. Druckmann *et al.*, "A high-performance speech neuroprosthesis," *Nature*, vol. 620, no. 7976, pp. 1031–1036, 2023.

[6] D. Dash, A. Wisler, P. Ferrari, E. M. Davenport, J. Maldjian, and J. Wang, "Meg sensor selection for neural speech decoding," *IEEE Access*, vol. 8, pp. 182 320–182 337, 2020.

[7] D.-Y. Lee, M. Lee, and S.-W. Lee, "Classification of imagined speech using siamese neural network," in *2020 IEEE International Conference on Systems, Man, and Cybernetics (SMC)*, 2020.

[8] A. Kamble, P. H. Ghare, and V. Kumar, "Deep-learning-based bci for automatic imagined speech recognition using spwvd," *IEEE Transactions on Instrumentation and Measurement*, vol. 72, 2023.

[9] S.-H. Lee, M. Lee, and S.-W. Lee, "Neural decoding of imagined speech and visual imagery as intuitive paradigms for bci communication," *IEEE Transactions on Neural Systems and Rehabilitation Engineering*, vol. 28, no. 12, pp. 2647–2659, 2020.

[10] L. Zhang, Y. Zhou, P. Gong, and D. Zhang, "Speech imagery decoding using eeg signals and deep learning: A survey," *IEEE Transactions on Cognitive and Developmental Systems*, vol. 17, no. 1, pp. 22–39, 2025.

[11] J. Tang, J. Chen, X. Xu, A. Liu, and X. Chen, "Imagined speech reconstruction from neural signals—an overview of sources and methods," *IEEE Transactions on Instrumentation and Measurement*, vol. 73, pp. 1–21, 2024.

[12] M. Rekrut, M. Sharma, M. Schmitt, J. Alexandersson, and A. Krüger, "Decoding semantic categories from eeg activity in silent speech imagination tasks," in *2021 9th International Winter Conference on Brain-Computer Interface (BCI)*, 2021, pp. 1–7.

[13] D. Lopez-Bernal, D. Balderas, P. Ponce, and A. Molina, "Exploring inter-trial coherence for inner speech classification in eeg-based brain–computer interface," *Journal of Neural Engineering*, vol. 21, no. 2, p. 026048, 2024.

[14] M. Haresh and B. S. Begum, "Towards imagined speech: Identification of brain states from eeg signals for bci-based communication systems," *Behavioural Brain Research*, vol. 477, p. 115295, 2025.

[15] A. Mohan and R. Anand, "Classification of imagined speech signals using functional connectivity graphs and machine learning models," *Brain Topography*, vol. 38, no. 2, pp. 1–18, 2025.

[16] J. T. Panachakel, A. Ramakrishnan, and T. Ananthapadmanabha, "Decoding imagined speech using wavelet features and deep neural networks," in *2019 IEEE 16th India Council International Conference (INDICON)*, 2019, pp. 1–4.

[17] L. Zhang, Z. Zhou, Y. Xu, W. Ji, J. Wang, and Z. Song, "Classification of imagined speech eeg signals with dwt and svm," *Instrumentation*, vol. 9, no. 2, 2022.

[18] W. Ting, Y. Guo-Zheng, Y. Bang-Hua, and S. Hong, "Eeg feature extraction based on wavelet packet decomposition for brain computer interface," *Measurement*, vol. 41, no. 6, pp. 618–625, 2008.

[19] B. C. Committee, "2020 international bci competition," Jul 2022. [Online]. Available: osf.io/pq7vb

[20] M. Rekrut and A. Mohamed Selim, "Eeg data recorded during spoken and imagined speech interaction with a simulated robot," Jan. 2025. [Online]. Available: https://doi.org/10.5281/zenodo.14645653

[21] J. Iriarte, E. Urrestarazu, M. Valencia, M. Alegre, A. Malanda, C. Viteri, and J. Artieda, "Independent component analysis as a tool to eliminate artifacts in eeg: a quantitative study," *Journal of clinical neurophysiology*, vol. 20, no. 4, 2003.

[22] R. W. Thatcher, "Coherence, phase differences, phase shift, and phase lock in eeg/erp analyses," *Developmental neuropsychology*, vol. 37, no. 6, pp. 476–496, 2012.

[23] K. Q. Lepage and S. Vijayan, "The relationship between coherence and the phase-locking value," *Journal of Theoretical Biology*, vol. 435, pp. 106–109, 2017.

[24] S. Duraisamy, M. Dubiel, M. Rekrut, and L. A. Leiva, "Transfer learning for covert speech classification using eeg hilbert envelope and temporal fine structure," in *ICASSP 2025*, 2025.

[25] D. Saravanakumar and M. R. Reddy, "A high performance hybrid ssvep based bci speller system," *Advanced Engineering Informatics*, vol. 42, 2019.

[26] A. Zandbagleh, S. Mirzakuchaki, M. R. Daliri, A. Sumich, J. D. Anderson, and S. Sanei, "Graph-based analysis of eeg for schizotypy classification applying flicker ganzfeld stimulation," *Schizophrenia*, vol. 9, no. 1, p. 64, 2023.

[27] U. Kriegel, "Perception and imagination: A sartrean account," in *Pre-reflective Consciousness*. Routledge, 2015, pp. 245–276.

[28] S. Haddad, K. Latifzadeh, S. Duraisamy, J. Vanderdonckt, O. Daassi, S. Belghith, and L. A. Leiva, "Good guis, bad guis: Affective evaluation of graphical user interfaces," in *Proceedings of the 32nd ACM Conference on User Modeling, Adaptation and Personalization*, 2024.

[29] R. Y. Lim, W.-C. L. Lew, and K. K. Ang, "Review of eeg affective recognition with a neuroscience perspective," *Brain Sciences*, vol. 14, no. 4, 2024.

[30] A. Kamble, P. H. Ghare, V. Kumar, A. Kothari, and A. G. Keskar, "Spectral analysis of eeg signals for automatic imagined speech recognition," *IEEE Transactions on Instrumentation and Measurement*, vol. 72, pp. 1–9, 2023.

[31] V. R. Carvalho, E. M. A. M. Mendes, A. Fallah, T. J. Sejnowski, L. Comstock, and C. Lainscsek, "Decoding imagined speech with delay differential analysis," *Frontiers in Human Neuroscience*, vol. 18, 2024.

[32] K. Alarabi Aljribi, "A comparative analysis of frequency bands in eeg based emotion recognition system," in *The 7th International Conference on Engineering & MIS 2021*, ser. ICEMIS'21. Association for Computing Machinery, 2021.

[33] G. A. P. Coretto, I. E. Gareis, and H. L. Rufiner, "Open access database of eeg signals recorded during imagined speech," in *12th International Symposium on Medical Information Processing and Analysis*, vol. 10160. SPIE, 2017.

[34] D.-Y. Lee, M. Lee, and S.-W. Lee, "Decoding imagined speech based on deep metric learning for intuitive bci communication," *IEEE Transactions on Neural Systems and Rehabilitation Engineering*, vol. 29, 2021.

[35] P. Dhananjaya, I. Adikari, S. Lakmali, I. Devindi, S. Liyanage, M. Wickramasinghe, T. Dissanayake, R. Ragel, and I. Nawinne, "Eeg based brain-computer interface for inner speech classification," in *2024 Moratuwa Engineering Research Conference (MERCon)*, 2024.